# Torsional wave band gap properties in a circular plate of a two-dimensional generalized phononic crystal

Lei Zhao, Haisheng Shu, Shanjun Liang, Xiaona Shi, Shuowei An, Wanyue Ren, and Jie Zhu

Citation: AIP Advances **8**, 055317 (2018); doi: 10.1063/1.5027600
View online: https://doi.org/10.1063/1.5027600
View Table of Contents: http://aip.scitation.org/toc/adv/8/5
Published by the American Institute of Physics

# Torsional wave band gap properties in a circular plate of a two-dimensional generalized phononic crystal

Lei Zhao,[1] Haisheng Shu,[1,a] Shanjun Liang,[2] Xiaona Shi,[1] Shuowei An,[1] Wanyue Ren,[1] and Jie Zhu[2,a]

[1]*Harbin Engineering University, Mechanical & Electrical Engineering College, 150001 Harbin, China*

[2]*The Hong Kong Polytechnic University, Department of Mechanical Engineering, Hung Hom, Kowloon, Hong Kong SAR, China*

(Received 4 March 2018; accepted 8 May 2018; published online 18 May 2018)

The torsional wave band gap properties of a two-dimensional generalized phononic crystal (GPC) are investigated in this paper. The GPC structure considered is consisted of two different materials being arranged with radial and circumferential periodicities simultaneously. Based on the viewpoint of energy distribution and the finite element method, the power flow, energy density, sound intensity vector together with the stress field of the structure excited by torsional load are numerically calculated and discussed. Our results show that, the band gap of Bragg type exists in these two-dimensional composite structures, and the band gap range is mainly determined by radial periodicity while the circumferential periodicity would result in some transmission peaks within the band gap. These peaks are mainly produced by two different mechanisms, the energy leakage occurred in circumferential channels and the excitation of the local eigenmodes of certain scatterers. These results may be useful in torsional vibration control for various rotational parts and components, and in the application of energy harvesting, etc.  https://doi.org/10.1063/1.5027600

## I. INTRODUCTION

The traditional theory of phononic crystals becomes more and more mature in recent years which makes the concept of phononic crystal show great application prospect in relevant fields such as elastic wave control, sound and vibration reduction etc.[1–3] More recently, the quasi periodic structures receive people's attention.[4,5] It has been manifested that band gap of elastic wave can also be produced by these special structures.[6–8] And not only that, some new properties may be in existence, for example, the phenomenon of energy localization in a circular phononic/photonic crystal without defect.[9,10]

As a part of the quasi periodic structures, we have extended the traditional concept of phononic crystal to a more general case, i.e., the generalized phononic crystal.[11] Through the investigation of a GPC plate and cylindrical shell with radial periodicity only, similar phononic band gaps are manifested numerically and experimentally.[11–13] It should be noted that, the frequently-used Bloch theorem is not applicable to these special structures involving material periodicities along curvilinear coordinates.[14–16] To characterize the band gap behaviors and wave propagation properties in those structures with one dimensional periodicity (radial periodicity), it is more suitable to combine the transfer matrix method and the concept of localized factor.[17–20]

In this paper, we will further consider the two-dimensional case of the GPC structure consisting of two different materials arranged periodically both in radial and circumferential directions. Due to the facts that the Bloch theorem and transfer matrix method are not applicable any more, the way of energy analysis is taken here to explore the band gap behaviors and the main physical quantities

[a]Authors to whom correspondence should be addressed. Electronic mail: shujs@hrbeu.edu.cn/jie.zhu@polyu.edu.hk

 

involved are power flow, energy density, and sound intensity vector, which are widely used in dynamic response analysis of general structures.[21–25]

The paper is organized as follows. The two-dimensional GPC model is presented in Section II together with a brief introduction of our analysis method. The numerical results of several typical cases are given based on which the existence and forming mechanism of the band gap are discussed in Section III. In Section IV, the non-peak frequency points in the band gap are investigated from the angle of energy distribution, which further demonstrates the effect of Bragg reflecting cancellation in the band gap. The peak frequency points in the band gap are then discussed in Section V in detail. Two main forming mechanisms are found and illustrated. Finally, the conclusions are given in Section VI.

## II. MODEL AND METHOD

The model of the GPC is given in Fig. 1 with the matrix and scatterers being distinguished by different colors. The scatterers are periodically arranged in the matrix both along the radial and circumferential directions. $\theta_1$ and $\theta_2$ are the angles occupied by the scatterer and circumferential channel respectively with $a_\theta = \theta_1 + \theta_2$ being the circumferential periodic constant. The radial size and spacing of the scatterers are represented by $a_1$ and $a_2$, and $a_r = a_1 + a_2$ is then the radial periodic constant.

The regions of these scatterers can be characterized as:

$$\begin{aligned} &r_0 + (n\text{-}1)a_r + a_2 \le r \le r_0 + na_r, n = 1, 2, \cdots n_r; \\ &\theta_0 + na_\theta \le \theta \le \theta_0 + (n+\gamma_\theta)a_\theta, n = 1, 2, \cdots n_\theta; \end{aligned} \tag{1}$$

where $r_0$ is the radius of the center hole, $n_r$ and $n_\theta$ are the numbers of radial and circumferential periodicities respectively, $\gamma_\theta = \theta_1/a_\theta$ is the filling ratio in the circumferential direction. In the following, the set of model parameters ($a_r$, $a_\theta$, $a_1$, $\theta_1$) will be used to represent the GPC model. Note that $n_\theta$ is determined only by $a_\theta$, i.e., $n_\theta = 360/a_\theta$, Fig. 2 shows four modes of GPCs in different model parameters.

For phononic crystals, the effect of band gap has been recognized as providing significant attenuation to those elastic waves whose frequencies fall in the gap. Essentially, the band gap effect can be understood and evaluated from the viewpoint of energy transmission since the wave propagation is actually the process of energy transmission.[26,27] Based on this knowledge, we can introduce some

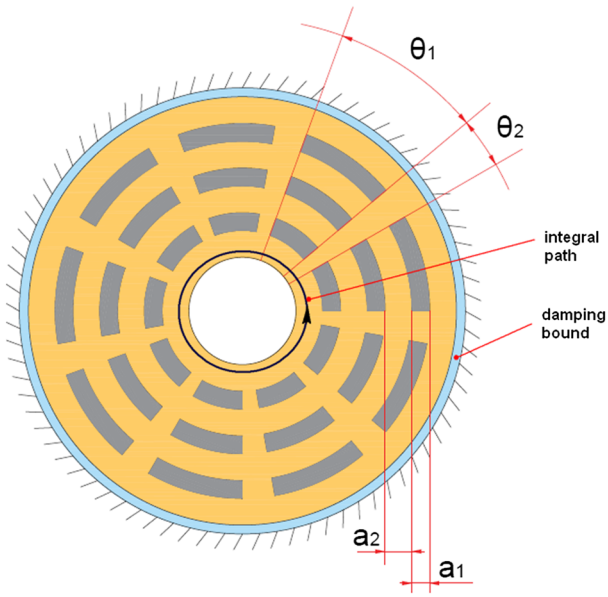


FIG. 1. GPC model.

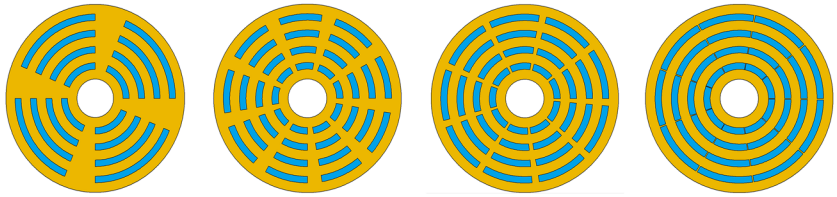

FIG. 2. The four GPCs modes of different structure parameters.

physical quantities relating to wave energy in the GPC analysis to investigate the wave energy flow and its distribution, instead of using traditional methods commonly used in the field of phononic crystals such as the energy band structure analysis based on the Bloch theorem which is not applicable for the case discussed in this paper. Here, the input power flow is taken to evaluate the suppression effect of the GPC structure on the torsional wave excitations within the whole interested frequency band, the mechanical energy density is used to investigate the energy distribution under certain frequencies, and the sound intensity vector is adopted to characterize the scenarios of energy flow occurred in different GPC models.

As presented in Fig. 1, we have applied a harmonic excitation of tangential displacement at the inner boundary to excite the torsional excitation as an energy source, and set the damping in the outer boundary as an energy absorber in the model to make sure the energy flowing through the undamped GPC structure. The loss factor and spring stiffness are set as 0.1 and N/$m^3$ in the outer boundary in order to keeping the free reflection boundary.

The in-plane wave motion excited by the stimulation at the inner boundary can be described as:

$$\mu\nabla^2\boldsymbol{u} + (\lambda+\mu)\nabla\nabla\cdot\boldsymbol{u} + \rho\boldsymbol{f} = \rho\ddot{\boldsymbol{u}} \tag{2}$$

Considering the complexity of the wave field, finite element method is adopted here to calculate the displacement and stress distributions within the structure, after which relevant physical quantities are then obtained. For the sound intensity vector, the components are given by:

$$\begin{aligned} I_x &= -\frac{\omega}{2}\,\mathrm{Re}\left(\sigma_x u_x^* + \tau_{xy} u_y^*\right) \\ I_y &= -\frac{\omega}{2}\,\mathrm{Re}\left(\sigma_y u_y^* + \tau_{xy} u_x^*\right) \end{aligned} \tag{3}$$

where Re denotes the real part and the symbol and * represents conjugate operation.

The power flow can be calculated by the integral of the sound intensity vector along a close path surrounding the excitation source, i.e.:

$$\begin{aligned} W &= \oint_l \boldsymbol{I}\cdot\boldsymbol{r}\cdot h\,ds \\ \boldsymbol{I} &= I_x\boldsymbol{i} + I_y\boldsymbol{j} \end{aligned} \tag{4}$$

where $l$ is the integral path that has been shown in Fig. 1, and $\boldsymbol{r}$ represents the unit normal vector of the point on the path.

## III. EXISTENCE AND FORMING MECHANISM OF THE BAND GAP

To facilitate following discussion, the material of the matrix is selected here as plastic for which the Young's modulus is $0.22 \times 10^{10} Pa$, poisson's ratio 0.375 and density 1190 $kg/m^3$, the material of the scatterers is assumed as lead whose Young's modulus, poisson's ratio and density are $4.08 \times 10^{10} Pa$, 0.3691 and 11600 $kg/m^3$, respectively.

The result of the power flow calculation for a GPC with four radial periods and geometry parameters specified as Fig. 2a is depicted in Fig. 3, together with the result of corresponding homogeneous structure made of plastic material. It can be seen that, there has no obvious frequency band with attenuation for the homogeneous case and the distribution of the peaks is nearly uniform on the whole. For the GPC case, however, significant reduction of power flow occurs within the reduced frequency

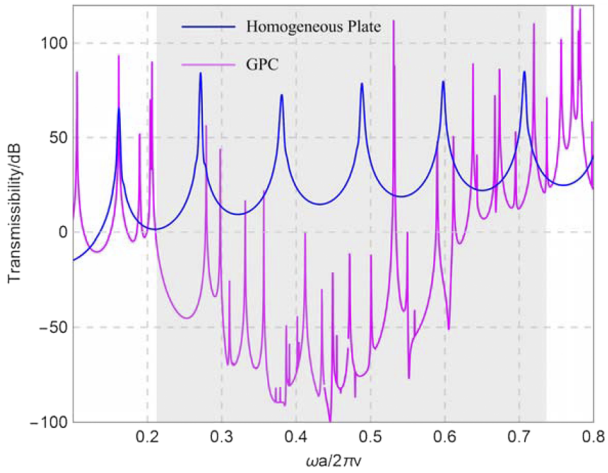


FIG. 3. Power flow curves of a specified GPC case and corresponding homogeneous structure.

region of 0.213-0.745, illustrating that the energy transmission would be suppressed quite a lot when the wave frequency falls in this region. Hence, it manifests that the wave band gap does exist in these special two-dimensional phononic crystals and the torsional wave excitation of frequency located in the gap can be effectively isolated from spreading outwards.

We have considered three other GPC models with different circumferential filling ratios, i.e., b—(50, 40, 20, 30), c—(50, 40, 20, 35) and d—(50, 40, 20, 39), for which the scatterer's angle and the circumferential periodic constant are 30/40, 35/40 and 39/40, respectively. The results of power flow calculation for these cases are given in Fig. 4, together with a limiting case where the circumferential filling ratio equals to 1, namely, the case of one-dimensional R mode having been analyzed in our previous paper. From Fig. 4, it can be observed that the power flow curves of the three GPCs have similar decay behavior within a common frequency band (0.195-0.805) which is basically the same as the case of one dimensional R mode. Apart from this, however, special features occur in the cases of GPCs when compared to the limiting case, i.e., there exist many peaks in the band gap region which may impair the wave attenuation effects.

The common frequency band gap of the above different GPCs including the limiting case can be understood from the internal forming mechanism. Despite of different circumferential filling ratios,

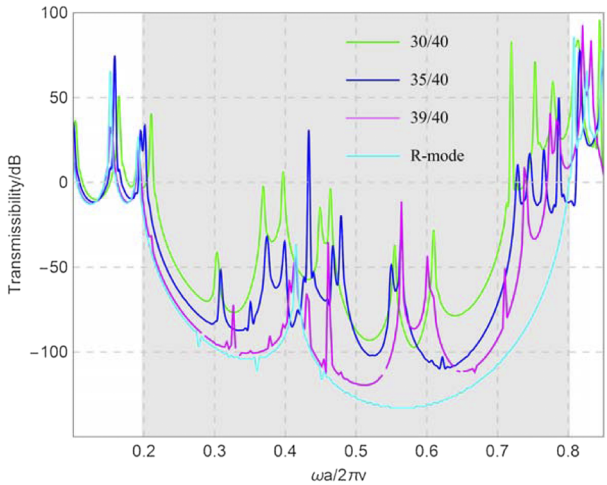


FIG. 4. Comparison of power flow curves for three different GPCs and a limiting case (one dimensional R mode).

i.e., different circumferential distributions, the radial periodic parameters are exactly the same in between these cases. Therefore, similar continuous reflecting cancellations may be formed at each radial interface, hence leading to similar behaviors of band gap. The Bragg type of these band gaps can also be verified from the match between the center frequency value and the wave length. Actually, according to the mechanism of Bragg reflection cancellation, the center reduced frequency of the first band gap is usually estimated to be around 0.5, which is obviously in accordance with the values found in Fig. 4. Now we have reason to believe that the wave band gap of the GPC model is mainly determined by its radial periodic arrangement. Nevertheless, the influences of the circumferential periodic distribution on the band gap behavior should not to be overlooked. In fact, the peaks occurred in the power flow curves are just the direct result of the circumferential periodic distribution, which will be discussed in the following.

## IV. ENERGY DISTRIBUTION AND FLOW AT NON-PEAK FREQUENCY IN THE BAND GAP

In this section, the frequency responses of the GPC model excited at non-peak frequency point located in the band gap are considered from the angle of energy distribution and flow by using sound intensity vector and energy density analyses. The case of peak frequency excitation will be discussed in next section.

The geometry parameter of the GPC considered here is the same as that used previously, i.e., Fig. 2a with four radial periods. Two non-peak frequency points in the band gap, 0.2561 and 0.3750 (please refer to Fig. 3), are calculated to obtain corresponding energy distributions which have been depicted in Fig. 5. It can be observed clearly that, the mechanical energy is located mainly in the matrix at the vicinity of inner ring where the excitation is loaded and the energy density decreases rapidly as the distance to the center increases. The energy field vanishes within almost all the part of the model apart from the internal region surrounded by the innermost scatterers, illustrating directly the strong effect of Bragg scattering cancellation in the band gap.

The energy distribution can be observed more detailedly by calculating the sound intensity vector at certain frequencies. As shown in Fig. 6a, the sound intensity vectors of the homogeneous case radiate evenly in the whole structure when excited at the reduced frequency of 0.2561, meaning that the energy of the source flows normally and evenly from inner to outer of the structure. The results of the GPC structure at two frequencies (0.2561 and 0.3750) within the band gap are depicted in Fig. 6b and Fig. 6c. It is observed that the sound intensity vector distributions of both frequencies are quite similar. The sound intensity vectors concentrate mainly at the vicinity of the excited region with large amplitude while distribute sparsely with small amplitude in other regions far from the center, which is in accordance with the distribution of energy density presented in Fig. 5.

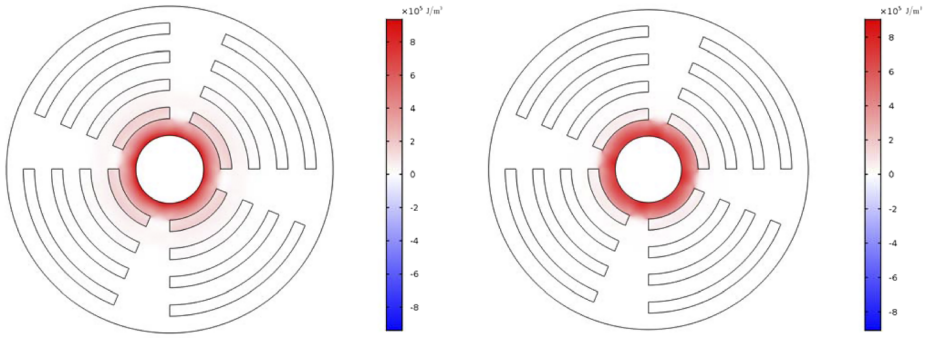


(a) (b)

FIG. 5. Energy distributions of a GPC structure with four radial periods and (50, 90, 20, 67.5) when excited at the inner boundary at two frequencies located in the band gap: (a) reduced frequency is 0.2561; (b) reduced frequency is 0.3750.

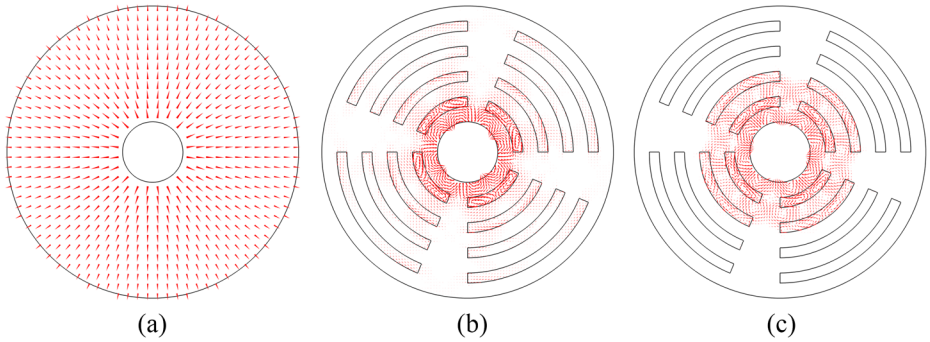


FIG. 6. Sound intensity field at non-peak frequency point located in the band gap (unit: $W/m^2$): (a) the homogeneous structure, the reduced frequency is 0.2561; (b) the GPC structure, 0.2561; (c) the GPC structure, 0.3750.

## V. ENERGY DISTRIBUTION AND FLOW AT PEAK FREQUENCY IN THE BAND GAP

The same GPC structure used in previous section is discussed here to investigate the properties of these peak frequencies in the band gap. By calculating and analyzing corresponding energy distributions of these peaks, two main forming mechanisms can be recognized. In the first case, the mechanical energy distributes mainly in the regions of circumferential channel formed by the matrix material, while in the regions formed by the matrix and scatterers the energy concentrates in the part close to the inner boundary. Significant from the first case, the mechanical energy focuses in certain scatterers only in the second case, and nearly no energy could be found in other regions, including other scatterers and the matrix.

The first case is investigated and discussed firstly with a typical peak frequency point (0.5885) located in the band gap (see Fig. 3). Fig. 7 gives the calculated result of the energy density distribution when excited at the selected frequency (Fig. 7a), together with the result of a peak point of 0.1616 (Fig. 7b) which locates in the pass band for comparison purpose. It can be observed that, at the reduced frequency point of 0.5885, the energy field is rather weak in the sector regions formed by scatterers and matrix, except for the first radial period, illustrating directly the modulation effect (continuous reflecting cancellation) of radial periodic material parameters on the excited wave. However, some energy leakage will be formed within the circumferential channel made of the matrix material, where the modulation effect of the radial periodicity becomes relatively weak. This energy leakage is mainly influenced by the structural parameters of the channel and the wave frequency.

In fact, the channel in this case may be viewed as a sector plate approximately with fixed circumferential boundary conditions. Hence it is not hard to conceive that there will exist corresponding modes of energy transmission at a series of discrete frequencies. Generally speaking, due to the fact

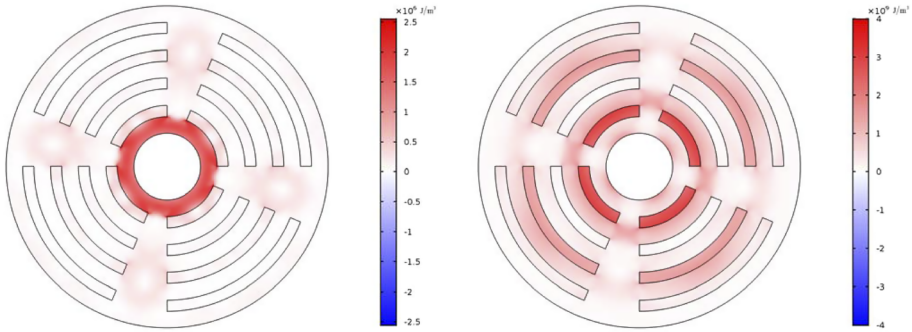


FIG. 7. Energy density distribution at the peak frequency point of (a) 0.5885 which is located in the band gap; (b) 0.1616 which is located in the pass band.

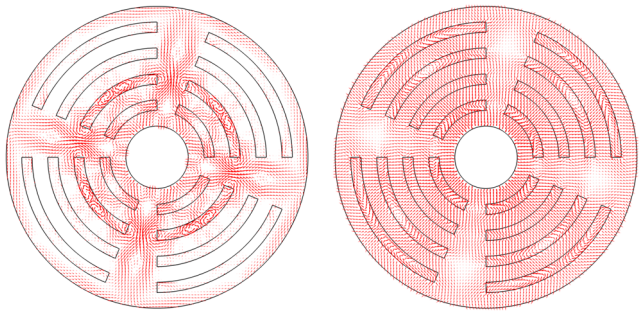


FIG. 8. Sound intensity vector distribution at the peak frequency point of. (a) 0.5885 which is located in the band gap and (b) 0.1616 which is located in the pass band (unit: $W/m^2$).

that the peak frequency point is still located in the band gap, the wave energy transmission will also decrease rapidly along the radial direction when excited at the vicinity of this frequency. In contrast, as shown in Fig. 7b, significant energy distribution can be found in almost all of the structure, owing to the peak frequency point is located in the pass band and hence no continuous reflecting cancellation could be formed by the radial periodicity.

We further calculate the vector field of sound intensity related to the peak frequency points mentioned above. As can be seen more clearly in Fig. 8a, the vector field concentrates mainly in the circumferential channels at the reduced frequency of 0.5885, demonstrating that the main energy provided by the excitation at the inner boundary flows outwards through these regions. Within the remained regions, i.e., those occupied by the scatterers and matrix with radial periodic arrangement,

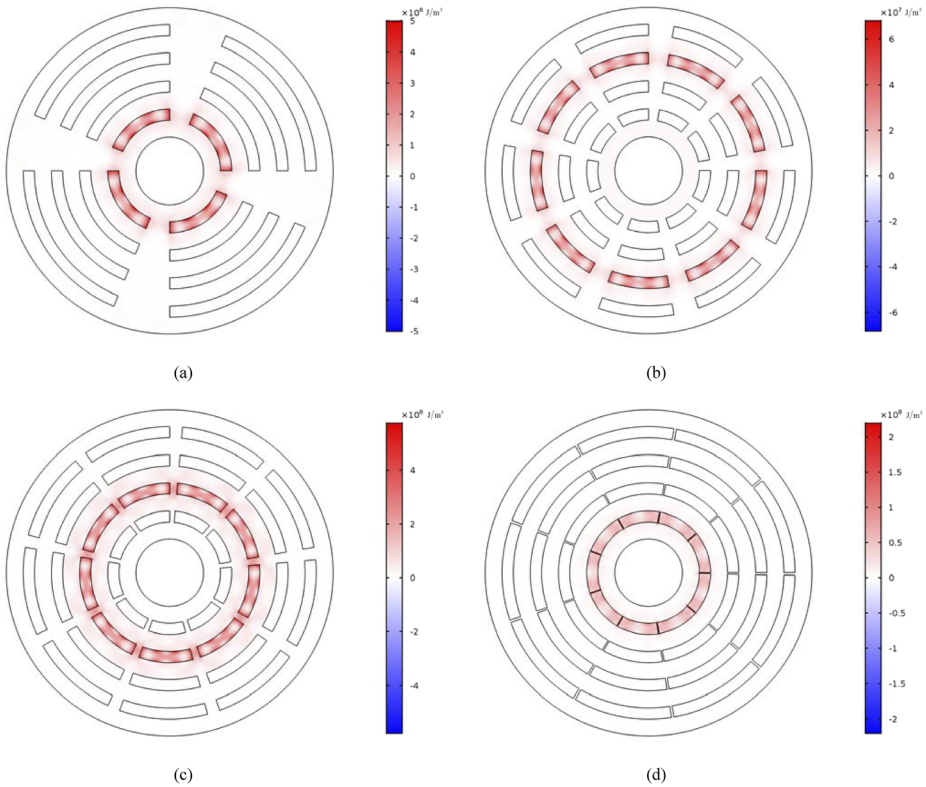


FIG. 9. Energy distribution of the GPC structure with four radial periods when excited at peak frequency in the band. gap: (a) Fig. 2a, 0.5305; (b) Fig. 2b, 0.6092; (c) Fig. 2c, 0.7293; (d) Fig. 2d, 0.6037.

the sound intensity vector field shows rapid and significant attenuation, which is just the result of the Bragg reflecting mechanism. In comparison with the peak point in the band gap, the sound intensity vector field corresponding to the peak point (0.1616) in the pass band is quite different as can be observed in Fig. 8b. The vector field has a densely distribution in all regions of the structure which means that the torsional wave energy can radiate from inner to outer through these regions without any resistance.

In the following, we will discuss the second case by using the same GPC structure. A typical peak frequency point (0.5305) is taken as an example to shed the light on the second forming mechanism of the peaks in the band gap. The energy distribution corresponding to this peak point is calculated and depicted in Fig. 9a. Very different from that of the first case presented above, the energy distribution in this case has shown a special pattern, i.e., energy focuses significantly within the four scatterers near the inner boundary and almost no energy could be found in all remained regions. In other words, highly localization of mechanical energy comes into being in this case. Other three GPCs are further investigated with different parameters: Fig. 2b, Fig. 2c and Fig. 2d, which have been treated in Section III (please see Fig. 4). As expected, the common feature or behavior of highly energy localization is also found in these different GPCs, which has been embodied in Fig. 9b–d.

To reveal the internal mechanism of the phenomenon of highly energy localization, the mises stress field distributions are further calculated aiming these peak frequency points related to the four GPCs, as shown in Fig. 10. Just as the distribution patterns of the mechanical energy and more clearly, the mises stress is also found to be concentrated in corresponding scatterers with certain regularity. The feature of highly concentration of energy and stress in the same discrete scatterers enlightens us that the main reason behind it is probably associated with the eigenmodes of these scatterers and has nothing to do with the two dimensional periodicities. To verify the idea, single scatterers with highly stress localized are extracted and treated individually. The eigenmodes of them are calculated at the vicinity of corresponding peak frequencies considered before, where the boundary conditions are set

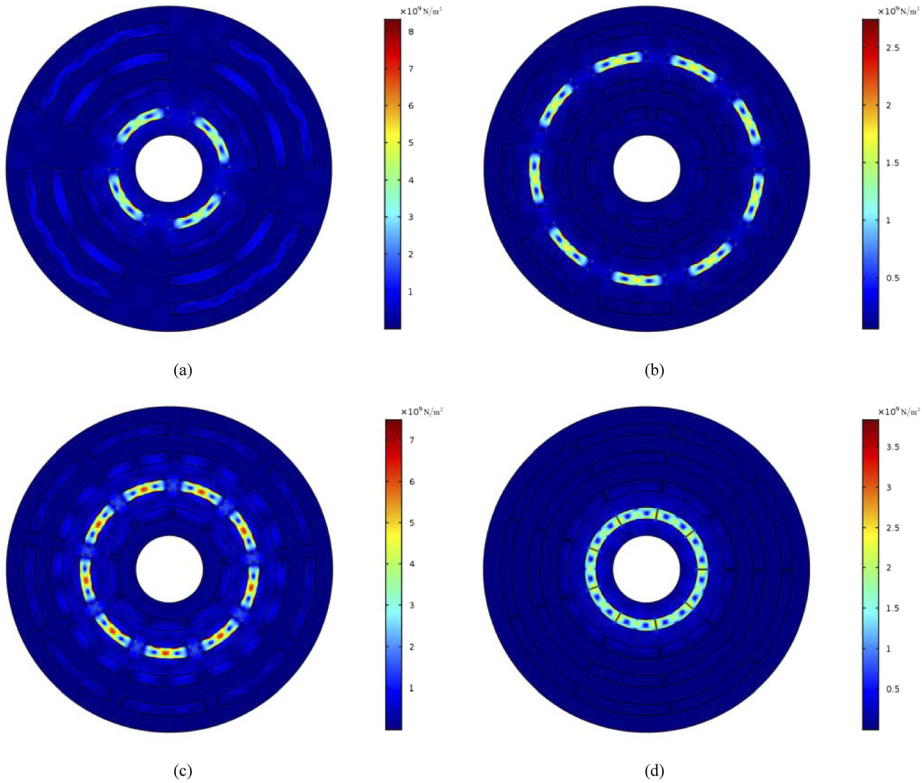


FIG. 10. Mises stress distribution of the GPC structure with four radial periods when excited at peak frequency in the band gap: (a) Fig. 2a, 0.5305; (b) Fig. 2b, 0.6092; (c) Fig. 2c, 0.7293; (d) Fig. 2d, 0.6037.

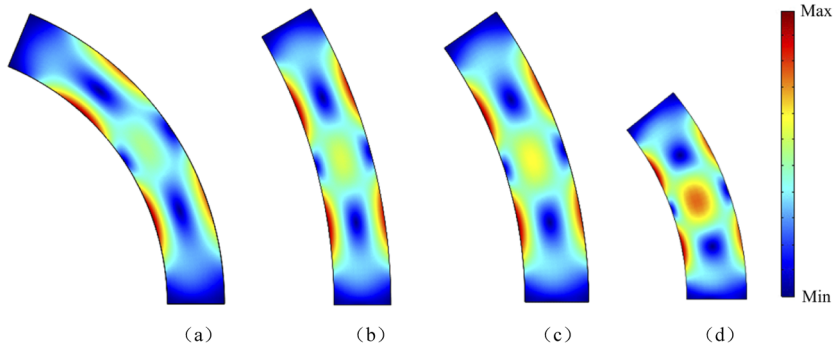


FIG. 11. Eigenmodes of the scatterers: (a) the scatterer on the first ring in Fig. 10(a) with angle/radial size are 67.5/20 and the eigen frequency is around 0.5361; (b) the scatterer on the third ring in Fig. 10(b) with angle/radial size are 30/20 and the eigen frequency is around 0.6155; (c) the scatterer on the second ring in Fig. 10(c) with angle/radial size are 35/20 and the eigen frequency is around 0.7417; (d) the scatterer on the first ring in Fig. 10(d) with angle/radial size are 39/20 and the eigen frequency is around 0.6325.

as free-free on the top and bottom surfaces and elastically supported case at the side faces with the elastic constants of the matrix material. By comparison of Fig. 10 and Fig. 11, it can be observed that the stress patterns highly localizing in the scatterers of the GPCs are indeed in accordance with those distributions of corresponding eigenmodes possessed by individual scatterers, which reveals that the second case is resulted from the excitation of local eigenmodes of certain scatterers.

For the second case, two main effects may be produced due to the excitation of certain local eigenmodes of scatterers. The first one is the effect of energy localization, i.e., the energy input from the exciting source will be focused and confined strongly within certain space region. The second one is the amplification effect of vibration of the outer part of the structure. Different from the case of non-peak point in the band gap, the energy of the exciting source is migrated from the inner boundary to the scatterers which is equivalent to be deemed as a migration of the exciting position from inner to outer, hence the vibration level of the outer part of the structure will be enhanced which can be easily observed from the displacement transfer curves (not presented here).

## VI. CONCLUSIONS

A kind of GPC structure with both radial and circumferential periodicities is investigated from the angle of energy distribution in this paper. Dynamic model is presented and some important physical fields associated with energy such as the power flow, energy density and the sound intensity vector are calculated numerically using the finite element method. Based on the results obtained, the wave transmission in the structure is analyzed and discussed aiming at the torsional wave excitation. Our work shows that:

1) there exists wide Bragg band gap for the GPC structure the frequency range of which is mainly determined by the radial periodicity formed by alternatively arranged materials along the radial direction. Meanwhile, the circumferential periodicity has important influences on the band gap behavior which is mainly embodied in several transmission humps within the band gap.
2) there exist two main forming mechanisms of the transmission humps in the band gap. The first one is originated from the energy leakage along the circumferential channels through which the wave energy input from the torsional excitation at the inner boundary radiates dominantly, while few energy is confined near the inner ring of scatterers. The second one is resulted from the effective excitation of certain eigenmodes of the scatterers, where the wave energy and stress field will be strongly localized in these scatterers with corresponding eigen patterns and almost no energy distribution could be found in the remained regions.

The structure and band gap properties of the GPC proposed in this paper have potential applications in several engineering fields. For example, the wave attenuation provided by the band gap can be used in torsional vibration isolation of rotational parts and components which are very widely used

in mechanical engineering. Moreover, the feature of strong localization of energy and stress may be beneficial for the applications related to energy trapping and harvesting.

## ACKNOWLEDGMENTS

This work was funded by the project (grant number 51375105) supported by the National Natural Science Foundation of China, the project (grant number LBH-Q15029) supported by the Postdoctoral Scientific Research Developmental Fund of Heilongjiang Province of China, and the project (grant number E201418) supported by the Natural Science Foundation of Heilongjiang Province of China.

[1] Y. Pennec, J. O. Vasseur, B. Djafari-Rouhani *et al.*, "Two-dimensional phononic crystals: Examples and applications."
[2] H. Shu, S. Liu, D. Zhao *et al.*, "A combined sonic crystal rod of Bragg type with ability of vibration reduction in broad frequency band," Noise Control Eng. J. **60**(1) (2012).
[3] S. Yoo, Y. Jae Kim, and Y. Y. Kim, "Hybrid phononic crystals for broad-band frequency noise control by sound blocking and localization," Acoustical Society of America (2012).
[4] Y. Li, T. Chen, X. Wang, S. Li *et al.*, "Lamb wave band gaps in one-dimensional radial phononic crystal plates with periodic double-sided corrugations," Physica B **476**, 82–87 (2011).
[5] Z. Chai, D. Wang, W. Liu, and D. Kong, "Torsional wave propagation in a piezoelectric radial phononic crystals," Noise Control Engr. J **64**(1) (2016).
[6] T. Ma, T. Chen, X. Wang *et al.*, "Band structures of bilayer radial phononic crystal plate with crystal gliding," Journal of Applied Physics **116**(10), 104505P (2014).
[7] Y. Li, T. Chen, X. Wang *et al.*, "Propagation of Lamb waves in one-dimensional radial phononic crystal plates with periodic corrugations," Journal of Applied Physics **115**(5), 054907P (2014).
[8] Q. H. Wen, "The study of characteristics of sphere-radial phononic crystals," Advanced Materials Research **211**, 609–614P (2011).
[9] M. Zhang, W. Zhong, and X. Zhang, "Defect-free localized modes and coupled-resonator acoustic waveguides constructed in two-dimensional phononic quasicrystals," Journal of Applied Physics **111**, 104314 (2012).
[10] W. Zhong and Z. Xiangdong, "Localized modes in detect-free two-dimensional circular photonic crystals," Physical Review A **81**, 013805 (2010).
[11] X. Shi, H. Shu, J. Zhu *et al.*, "Research on wave bandgaps in a circular plate of radial phononic crystal," International Journal of Modern Physics B **30**, 1650162 (2016).
[12] H. Shu, L. Dong, S. Li *et al.*, "Propagation of torsional waves in a thin circular plate of generalized phononic crystals," Journal of Physics D: Applied Physics **47**(29) (2014).
[13] H. Shu, X. Wang, R. Liu *et al.*, "Bandgap analysis of cylindrical shells of generalized phononic crystals by transfer matrix method," International Journal of Modern Physics B **29**(24) (2015).
[14] D. Torrant and J. Sánchez-Dehesa, "Acoustic resonances in two-dimensional radial sonic crystal shells," New Journal of Physics **12**, 073034 (2010).
[15] D. Torrant and J. Sánchez-Dehesa, "Radial wave crystals: Radially periodic structures from anisotropic metamaterials for engineering acoustic or electromagnetic waves," Physical Review Letters **102**, 064301 (2009).
[16] Z. Xu, F. Wu, and Z. Guo, "Low frequency phononic band structures in two-dimensional arc-shaped phononic crystals," Physics Letters A **376**(33), 2256–2263 (2012).
[17] Y. Z. Wang, F. M. Li, W. H. Huang *et al.*, "The propagation and localization of Rayleigh waves in disordered piezoelectric phononic crystals," Journal of the Mechanics and Physics of Solids **56**(4), 1578–1590 (2008).
[18] F. M. Li, M. Q. Xu, and Y. S. Wang, "Frequency-dependent localization length of SH-wave in randomly disordered piezoelectric phononic crystals," Solid State Communications **141**(5), 296–301 (2007).
[19] L. I. Fengming, W. Yuesheng, H. Wenhu, and H. U. Chao, "Advances of vibration localization in disordered periodic structures," Advances in Mechanics **35**(4) (2005).
[20] Y. Zongjian and Y. Guilan, "Research on vibration mode localization in mistuned cyclic periodic structures," Science Technology and Engineering **5**(21) (2005).
[21] K. Min Swe, *Computational of structural intensity in plate* (The national university of Singapore, 2003).
[22] X. D. Xu, H. P. Lee, Y. Y. Wang, and C. Lu, "The energy flow analysis in stiffened plates of marine structures," Thin-Walled Structures **42**, 979–994 (2004).
[23] L. Gavric and G. Pavic, "A finite element method for computation of structural intensity by the normal mode approach," Journal of Sound and Vibration **164**(1), 29–43 (1993).
[24] W. Xianjun, Z. Shijian, and C. Jianhua, "Review on structural vibration power flow prediction methods," Advances in Mechanics **36**(3) (2006).
[25] W. Yong, X. Qing, H. Qibai, and L. Xiaozheng, "Study on power flows of vibration isolation system adopting finite periodic composite structure," China Mechanical Engineering **18**(22) (2007).
[26] M. Zhang, W. Zhong, and X. Zhang, "Defect-free localized modes and coupled-resonator acoustic waveguides constructed in two-dimensional phononic quasicrystals," Journal of Applied Physics **111**, 104314P (2012).
[27] W. Zhong and X. Zhang, "Localized modes in detect-free two-dimensional circular photonic crystals," Physical Review A **81**, 013805P (2010).